DIFFUSION STUDY OF NaCl AND KCl AT THE SOLUTION/OLIVE INTERFACE: MATHEMATICAL MODELING USING THE FINITE ELEMENT METHOD AND SELF-ORGANIZING FEATURE MAP (SOFM)-TYPE NEURAL NETWORKS

Dionisio Borsato[a,*, iD], **Marco A. J. Clemente**[a], **Heloisa H. P. Silva**[a], **Nathan F. Silva**[a], **Julia W. Campos**[a], **Eduardo G. de Sousa**[a], **Hágata C. Silva**[a], **Karina B. Angilelli**[a], **Ana C. G. Mantovani**[b, iD] **and Rafael G. Mantovani**[c]

[a]Departamento de Química, Universidade Estadual de Londrina (UEL), 86057-970 Londrina – PR, Brasil
[b]Centro Universitário Ingá (UNINGÁ), 87035-510 Maringá – PR, Brasil
[c]Universidade Tecnológica Federal do Paraná (UTFPR), 86812-460 Apucarana – PR, Brasil

Artigo

Olive samples were subjected to the salting process in brine containing 1196 mol m^{-3} of NaCl and 402 mol m^{-3} of KCl. Samples were collected during 60 h and salt concentration values were determined. With the finite element method (FEM) and the minimization of the errors percentage between the simulated and experimental values, the mass transfer coefficients in the film (h_m) were obtained, being 1.0072×10^{-8} and 1.2499×10^{-8} for NaCl and KCl, respectively. The salts concentration at the olive/brine interface was simulated by FEM and analyzed via SOFM. A network with 4×4 topology and 10000 training epochs was used. It was observed that the influence of the stationary film formed on the surface of the olives during the salting process depends on the position, the salt involved in the diffusion and that the concentration of the salts, at each point, varies according to the immersion time.

Keywords: self-organizing maps; NaCl; KCl; simulation; salt diffusion.

INTRODUCTION

Olives are one of the most cultivated and consumed fruits in Mediterranean countries and their products, olive oil, and table olives are relevant components of the population's diet and have great economic importance for producing countries. They are widely consumed throughout the world and lower the risk of heart disease and the incidence of certain types of cancer (breast and colon) is associated with this diet. Agronomic factors, the cultivar, the stage of maturation, and the processing method used are the main factors that influence the nutritional and non-nutritional composition of table olives and their organoleptic properties. The processing method of ripe olives includes storage in brine (5-10%) for 2 to 6 months. The production of natural olives in brine often consists in olives direct salting without any debittering treatment.[1-5]

Aiming for a healthier diet, many consumers have chosen to purchase foods with reduced sodium levels and due to the great interest in consuming these types of products, researches are being carried out to reduce or replace sodium chloride in foods while maintaining their sensory characteristics unchanged.[6-8] Potassium chloride has emerged as a partial substitute for sodium chloride due to its similar properties. It is considered antihypertensive since potassium intake increases renal sodium excretion and has antimicrobial action similar to that of sodium chloride.[7,9,10] It is possible to make this substitution because this salt, as reported in the literature, does not change the sensory, physical, or microbiological characteristics of the product. However, the total replacement of NaCl by KCl is not recommended because in concentrations above 30% it gives a bitter taste to the final product.[7,9,10]

To insert the salts in the olives it is necessary to carry out salting, which consists of immersing the fruit in brine, where the salt penetrates the solid through mass diffusion.[11,12] According to Cremasco *et al*.,[13] in the salting process, when a fluid is in contact with a solid, the formation of a film on its surface occurs, and to assess its influence on diffusion it is necessary to consider the ratio between the internal and external resistance that can be quantified by the Biot mass number.

According to Bona *et al*.,[14] and Angilelli *et al*.,[15] the increase in Biot number values indicates less influence of the surface barrier during mass transfer, with dominant internal resistance. During the diffusion process, as the Biot number decreases, there is a greater influence of the layer on the flow of ions at the interface, thus limiting the diffusion by external resistance. Hence, the Biot number is related to the film coefficient, since the higher its value the lower the influence of the film formed on the diffusion process. When it comes to food biosolids, surface diffusion and film formation may depend on the geometry and position where diffusion occurs.[13] The main mass transfer coefficient, the cross coefficients, and the relationship between the mass transfer coefficient and the mass conductivity are also parameters studied in the diffusion process that can be obtained using the finite element method (FEM), a methodology that generates numerical solutions from differential equations, simulating process under realistic conditions.[16]

For a better understanding of the parameters' effects during the diffusion process, such as diffusion and film coefficients and Biot number, some data analysis tools, such as artificial neural networks, which use unconventional statistics, can be used.[17,18]

There are several types of neural networks, among them, the Multilayer Perceptron Networks, Radial Basis, and Self-Organizing Feature Maps (SOFM) stand out. The SOFM network is a tool capable of processing data, transforming an input pattern of arbitrary size into a discrete one- or two-dimensional map.[18] SOFM performs this transformation in a topologically ordered way, based on an unsupervised learning algorithm.[17,19] This data mapping in neurons arrangement preserves topological relationships and the distribution probability, hence SOFM is a powerful tool for interpreting data. In this type of neural network, the result can be observed through a topological map whose function is to facilitate the visualization of clusters and also the neighborhood relationship between the formed groups. Close groups share some similarity and the greater the Euclidean distance, the greater the difference in behavior.[17]

*e-mail: dborsato@uel.br

The SOFM algorithm consists in a set of input data and a grid of connected computational neurons, which compete with each other for the activation of the one that most resembles the input vector.[18] If the input data show some similarity between the classes, the neurons will be organized among themselves, showing patterns of similarity in a grid, usually two-dimensional, rectangular or hexagonal. Mapping data onto the neuron matrix preserves topological relationships and distribution probability.[17]

These tools have been applied to solve various types of problems in different areas of science, such as engineering, chemistry, medicine, and bioenergy.[20-25] In food science, according to Boishebert *et al.*,[26] strawberry varieties, as well as other fruit species, can be characterized from their chemical composition and more precisely from their volatile components, using self-organizing map-type networks. Bona *et al.*[20] applied the SOFM in the post-processing of electronic nose data, of seven coffee varieties, and concluded that this methodology was a promising choice for the development of new products and quality control of soluble coffee. Cremasco *et al.*[17] applied the SOFM in the segmentation of soybean varieties and showed that the network was able to differentiate the samples according to the concentrations of inorganic components. Oliveira *et al.*[27] reported that the combination of SOFM with FEM simulation proved to be an appropriate tool, as a new application of prato cheese salting, to evaluate the formation of the film, showing that this phenomenon influences the mass transfer and diffusion time.

The objective of this work was to investigate the formation, influence, and behavior of the film during the NaCl and KCl diffusion in olives, applying artificial neural networks such as Self-Organizing Feature Maps with 3D computational modeling using the Finite Element Method.

EXPERIMENTAL

Olives

The olives used are of the Arbequina variety, produced in Ventania - PR, Brazil (24 06' 58" S, 50 11' 31" W) whose mean dimensions, measured with a digital pachymeter are shown in Figure 1a.

Brine preparation and sampling

12 L of brine with 402 mol m^{-3} of potassium chloride (30% w/v) and 1196 mol m^{-3} of sodium chloride (70% w/v) were used. The olive samples were completely immersed in the brine, without previous treatment, being collected at 0, 6, 12, 14, 15, 17, 18, 22, 25, 33, 39, 45, 51, 57, and 60 h. Each sample consisted of a set of pulps from three olives.
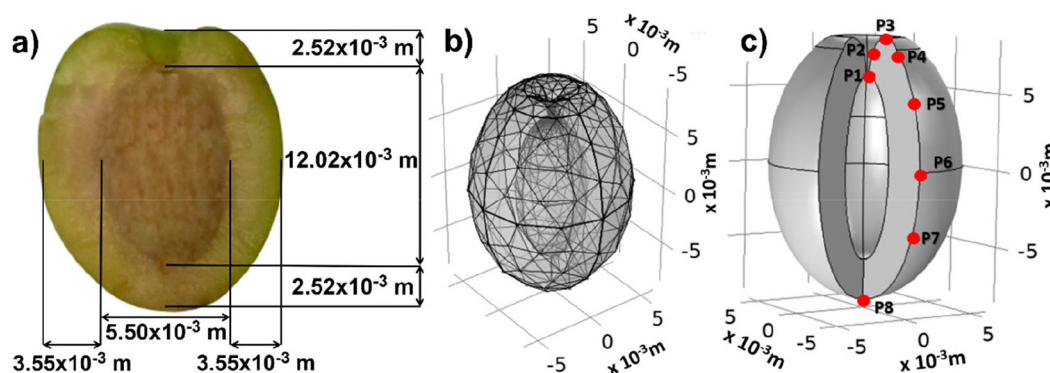
Determination of sodium and potassium chloride

The concentrations of NaCl and KCl in olive pulp samples were determined according to the methodology described by Bordin *et al.*,[7] with modifications, using the Micronal photometer, model B-462, with an air pressure of 0.8 kgf cm^{-2} and air pump pressure of 1.5 kgf cm^{-2} using butane gas.

Finite element method (FEM)

The mathematical modeling of the process by finite element method (FEM), was carried out considering a tetrahedral mesh (Figure 1b), simultaneous three-dimensional mass transfer of two solutes, and the hypothesis that the main diffusion coefficients (D_{11} and D_{22}), crossed (D_{12} and D_{21}) and the film mass diffusivity coefficient (h_m) were constant, regardless of the position and immersion time. Diffusion of solutes was considered the predominant process in the mobility of the ions and occurred under isothermal conditions of 20 ± 1 °C, with flow only in the olives' pulp, according to the boundary condition shown in Figure 1. The contraction of the samples during the procedure was considered negligible.

The concentrations of NaCl and KCl salts were represented respectively by C_1 (x, y, z, t) and C_2 (x, y, z, t) at a given point P (x, y, z) $\in$ to the domain (Ω) and in a definite time (t), in which they can be determined based on the Onsager equations.[28]

At the beginning of the diffusion process, the initial concentrations of NaCl and KCl in the olive were represented by $C_{1.0}$ and $C_{2.0}$, respectively, obeying the Cauchy boundary condition, that is, considering the presence of a resistive film at the interface of the biosolid/brine.[13]

The Biot number, which expresses the ratio between the internal and external mass transfer resistance, is related to the coefficient h_m, the mass conductivity (λ_m), and the characteristic dimension represented by the average thickness of the pulp, as shown in Figure 1a.[13,17]

Figure 1 shows the mean widths, heights, and pulp dimensions (a) as well as the mesh used in the simulation procedure by the FEM (b) and the points chosen on the olive surface to simulate the behavior of the film formed over time (c).

Data matrix

With the application of the MEF, the NaCl and KCl concentrations were determined at each point described in Figure 1c as a function of time, obtaining two data matrices, with dimensions of 9 × 154 for NaCl and 9 × 132 for KCl. The time interval used to simulate the concentration of each salt is described in Table 1.

Figure 1. *Mean dimensions of the olive (a), the mesh used (b), and points chosen on the surface to analyze the behavior of the film (c)*

Table 1. Time interval used to simulate the concentration of NaCl and KCl at each point described in Figure 1c

NaCl		KCl	
Time interval (h)	Time gradient (h)	Time interval (h)	Time gradient (h)
1-10	0.5	1-10	0.5
10-30	1	10-30	1
30-100	5	30-100	5
100-400	10	100-400	10
400-4700	100	400-5300	100
4700-6800	300	5300-7400	300

The choice of time intervals is not arbitrary but is aimed at adequate data collection to ensure the best network performance. The application of a very wide time gradient in the initial times can result in errors that will propagate throughout the simulation period. Thus, smaller gradients are used at the beginning of the analysis, because, at this moment, the greatest concentration changes occur. As time goes by and the balance of salt concentration at the biosolid/brine interface approaches, the concentration variation rate becomes smaller and, therefore, the use of larger gradients becomes more appropriate, optimizing the computational processing time.

Artificial neural networks (ANN)

The SOFM network applied to each salt, in each system separately, consisted of a 4 × 4 hexagonal topology with 10000 training epochs. The initial neighborhood relationship was 1.0 with an initial learning rate of 0.2, decaying exponentially with training epochs to 0.928×10^{-4}. The procedures used to determine the topological neighborhood, the exponential decay, the adaptive process, the synaptic weight vector as well as the decrease in the learning rate, are described by Cremasco *et al.*[13,17] In order to assess similarities and divergences in the behavior of each point for each salt as a function of concentration variation over time, topological and weight maps were generated.

Computer processing

The computer program COMSOL Multiphysics® version 5.2 (COMSOL, Inc., Burlington, MA)[29] based on the finite element method was used for the simulation. The neural network routine used was developed according to the algorithm described in Haykin[18] and processed by the Matlab® R2007b (MathWorks, 2012)[30] software to evaluate the influence and behavior of NaCl and KCl concentrations in mol m^{-3} on the olive surface.

RESULTS AND DISCUSSION

To simulate the diffusion process of sodium and potassium chloride, the olives were immersed in brine for 60 h. During the salting period, samples were collected at each established time, which were composed of three olives. The dimensions of the olives were determined, the pulp was removed, weighed, and placed in porcelain crucibles to determine the moisture content and the sodium and potassium chloride concentration. At the beginning and end of the salting period, the concentrations of NaCl and KCl in the brine were determined. The final concentrations did not show a significant difference at the level of 5% when compared to the beginning of the salting process, because to keep the concentration of salts in the brine constant, the ratio between its volume and the volume occupied by the olives was 50:1.

To have a mass transfer across the olive surface, the flow must first pass through a stationary thin film along the interface, which acts as a resistive barrier, and therefore there is a specific diffusion coefficient that describes the mass transfer in this film. To evaluate the influence of the formed film, it is necessary to consider the ratio between the external and internal mass diffusivity resistance, which can be quantified by the mass Biot number. In addition to the resistance at the interface, the main and cross-diffusion coefficients are also important parameters in the diffusion process. These coefficients cannot be determined only experimentally, but by semi-empirical methods that use experimental data coupled to the diffusion simulation using the finite element method (FEM).[10] Table 2 shows the values of the coefficients obtained with the application of the FEM and simulated to minimize the percentage errors.

Table 2. Adjusted values for main and cross-diffusion coefficients, Biot number, and the film coefficient

	NaCl	KCl
Main diffusion coefficient (m^2 s^{-1})	0.4358×10^{-12} (D$_{11}$)	0.5408×10^{-12} (D$_{22}$)
Cross diffusion coefficient (m^2 s^{-1})	0.0293×10^{-12} (D$_{12}$)	0.0329×10^{-12} (D$_{21}$)
h$_m$ (m s^{-1})	1.0072×10^{-8}	1.2499×10^{-8}
Error (%)	5.35	4.77
Biot	82.05	

Adapted from Clemente *et al.*[31] Biot number estimated in relation to the *x*-axis. h$_m$: mass transfer coefficient.

With the values of the main and crossed diffusion coefficients and the mass transfer coefficients in the film (Table 2), the diffusion simulation by FEM at points P1 to P8 was performed. The concentration values of NaCl and KCl, in the different salting times, were tabulated in a 9 × 154 matrix for NaCl and 9 × 132 for KCl and processed using the SOFM neural network to analyze the diffusion of the salts through the film formed on the surface of the olive.

The SOFM network transforms an input pattern of arbitrary dimension into a discrete one- or two-dimensional map of neurons and performs its transformation adaptively in a topologically ordered way.[18] The map containing the results has the function of facilitating the clusters' visualization and also the neighborhood relationship between the formed groups, using a set of rules that serve as criteria for this purpose.[17,18,25]

The simplest way to evaluate the groups formed in a multidimensional space is through the determination of Euclidean distances. In the topological map, close groups share some similarities, also the greater the distance the greater the sharing difference. In the topological map, the groups' definition is characterized by the presence of empty neurons between the clusters. If the topology is too small for the database, the neighborhood relationship between all neurons can be so close that the network can classify all samples as a single cluster. If the network topology is very large, there is a large data dispersion, which can negatively affect the clustering of samples.[13,17,25]

Figure 2 shows the topological maps of NaCl and KCl obtained by the SOFM network, during 8000 and 7300 h of salting simulation, respectively, at points P1 to P8 on the olive surface (Figure 1c).

In the chosen 4 × 4 hexagonal topology, each neuron has 6 sides, therefore they can have a similarity with up to 6 other neurons. Since the characterization of the groups is based on the presence of empty neurons between the clusters, it can be concluded that the network was able to identify differences in salts concentrations in the diffusion

process concerning the geometry of the olive, which is one of the main factors for the difference in diffusion between the chosen points on the surface, as it is directly related to the formation, thickness and behavior of the film during the diffusion of the salt. However, in the topological map, the groups formed for sodium chloride and potassium chloride were not the same, indicating different behavior of the salts during diffusion through the film. Among the differences in the salts used is the value of the film coefficient (h_m) of KCl, which is 24% higher than that of NaCl, which can be explained by mobility in aqueous media, since Na^+ has a larger hydration radius, which causes lower mobility when compared to the K^+ ion.[32]

According to the topological map (Figure 2), NaCl formed 4 distinct groups and KCl showed a greater dispersion forming 5 groups. However, for both NaCl and KCl, points P4, P5, P7, and P8 showed similar diffusion behavior, indicating that the resistive barrier at these points on the surface is independent of the salt studied in the present work. The similarity in the diffusive behavior is greater when the points are grouped in the same neuron, as is the case of the points P4, P8, and P3, P6 superimposed on the NaCl topological map, but in different neurons and at the ends. Such behavior is not the same in the KCl map because the neurons where these points are located are not connected by the edges of the hexagons, but there is an overlap of points P5 and P7. The diffusion in P1, whose position has a large concavity and it is close to the stone (Figure 1c), did not show similarity with any other point in the olive for both the NaCl and KCl maps. The same behavior was observed at point P2 for both salts.

The weight map is a graph that presents contour regions with different colors for each weight plane. Samples that are in the region of the same color have the same weight and similarity. Together with the topological map, it is possible to extract behavior rules for each group formed, at each time of the salting process, and with that, to evaluate the influence of each variable on the results obtained.

Figures 3 and 4 show the weight maps obtained during the process of simulating the concentrations of NaCl and KCl during 6800 and 5100 h of olive salting, respectively. It is important to note that when evaluating the weight, at each analysis time, the network performs a normalization of the concentration values. Thus,
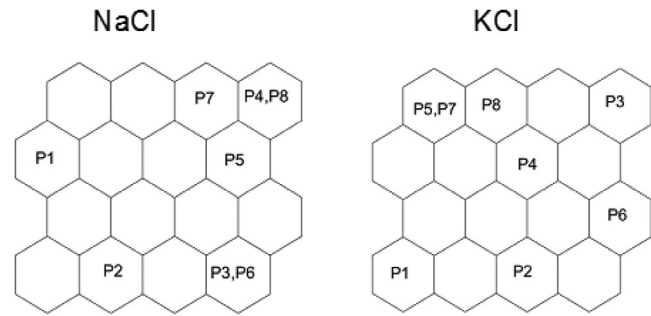

Figure 2. *Topological map showing the arrangement of the chosen points on the surface of the olive during the salting simulation*

although the different colors are related to similar concentration values in the caption, they indicate different weights. Points that are in the blue-colored region have a lower weight value, while those in yellow have a higher weight.

The points' position in the two figures is the same as the arrangement of the points shown in the topology (Figure 2). Figure 3 shows that at the beginning of the salting process (1 h) the concentration of sodium chloride on the surface of the olive pulp follows the sequence P1 > P2 > P3 $\cong$ P6 > P5 > P4 $\cong$ P8 > P7. However, after the first hour, at points P1 and P2, the rate at which the concentration increases are lower compared to the other points. This behavior may be related to the fact that it is a region where the pulp thickness is thinner, very close to the stone and due to the large concavity, the film may have taken longer to form. Once the film is established or has its thickness increased it naturally slows down the diffusion. From the second hour onwards, the highest concentrations of NaCl occur at points P3 and P6 and remain so until the sixth hour. From this time onwards, the highest concentration is verified at point P7 (40 h) and remains so until the end of the salting process. From 5400 h onwards, the concentration at all points is close to the value corresponding to the NaCl concentration in the brine, reaching the Dirichlet boundary condition[14] at 6800 h.

Figure 4 shows that at the beginning of the salting process (1 h) the concentration of KCl on the olive surface, at the chosen
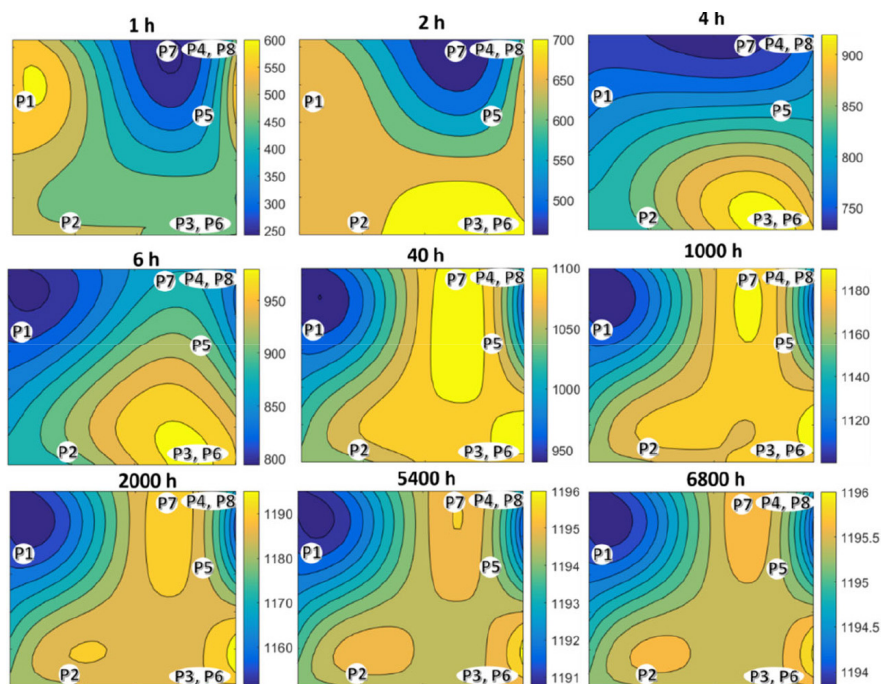

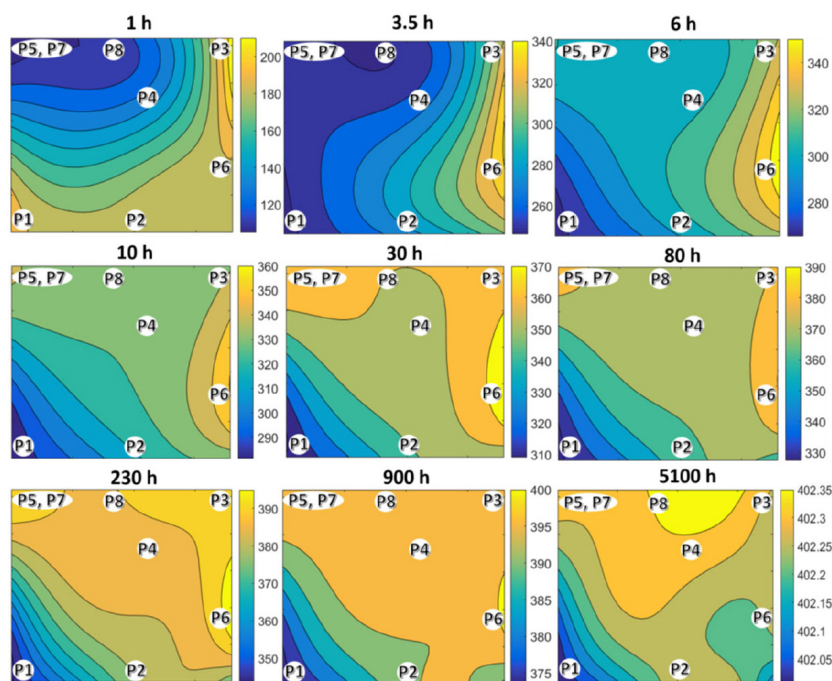**Figure 3.** *Weight map for the NaCl diffusion on the olive surface*

Figure 4. *Weight map for the KCl diffusion on the olive surface*

points (Figure 1c), from highest to lowest, follows the sequence P1 ≅ P3 > P2 ≅ P6 > P4 > P8 > P5 and P7. The same effects on the geometry and film formation of the P1 and P2 region discussed for NaCl apply to KCl. From 3.5 h to 6 h of salting, the highest concentrations of KCl are at points P3 and P6. In the sixth hour, points P2, P4, P5, P7, and P8 presented similar concentrations, and from that time on P1 starts to have the lowest concentration on the surface extending up to 5100 h. From 10 h of salting until the end of the process, the concentration at points P3, P5, and P7 are similar. Furthermore, from 10 h, points P4 and P8 remain similar to each other with intermediate concentrations, that is, not as low as the concentration in P1 and not as high as P6 until 900 h. It is important to highlight that point P8 is the first to reach the Dirichlet boundary condition.[14]

CONCLUSIONS

The application of the artificial neural network of the self-organizing maps type proved to be an efficient and easy-to-view tool to evaluate the behavior of the stationary film formed on the surface of the olive during the diffusion process by immersion in an aqueous solution.

The presence of a stationary film on the surface of the olive during the salting process, and the analysis of the topological and weights maps showed that the diffusion at the olive/solution interface varies according to the type of chemical species involved in the diffusion and to the geometry of the biosolid. The simulation by FEM combined with ANN of the SOFM type was an effective tool to evaluate this behavior as well as to modulate the salting time, which is very useful in the food industry.

ACKNOWLEDGMENTS

REFERENCES

1. Aydar, A. Y.; *Food Sci. Technol.* **2021**, *41*, 238. [Crossref]
2. López, A.; García, P.; Garrido, A.; *Food Chem.* **2008**, *106*, 369. [Crossref]
3. Magdich, S.; Abid, W.; Boukhris, M.; Rouina, B. B.; Ammar, E.; *Ecological Engineering* **2016**, *97*, 122. [Crossref]
4. Pereira, J. A.; Pereira, A. P. G.; Ferreira, I. C. F. R.; Valentão, P.; Andrade, P. B.; Seabra, R.; Estevinho, L.; Bento, A.; *J. Agric. Food Chem.* **2006**, *54*, 8425. [Crossref]
5. Rocha, J.; Borges, N.; Pinho, O.; *J. Nutr. Sci.* **2020**, *9*, e57. [Crossref]
6. Barat, J. M.; Baigts, D.; Aliño, M.; Fernández, F. J.; Pérez-García, V. M.; *J. Food Eng.* **2011**, *106*, 102. [Crossref]
7. Bordin, M. S. P.; Borsato, D.; Cremasco, H.; Galvan, D.; Silva, L. R. C.; Romagnoli, E. S.; Angilelli, K. G.; *Food Chem.* **2019**, *273*, 99. [Crossref]
8. Rodrigues, F. M.; Rosenthal, A.; Tiburski, J. H.; da Cruz, A. G.; *Food Sci. Technol.* **2015**, *36*, 1. [Crossref]
9. Bona, E.; Borsato, D.; da Silva, R. S. S. F.; Silva, L. H. M.; *Cienc. Tecnol. Aliment. (Campinas, Braz.)* **2005**, *25*, 394. [Crossref]
10. Borsato, D.; Moreira, M. B.; Moreira, I.; Pina, M. V. R.; da Silva, R. S. S. F.; Bona, E.; *Food Sci. Technol.* **2012**, *32*, 281. [Crossref]
11. Albarracín, W.; Sánchez, I. C.; Grau, R.; Barat, J. M.; *Int. J. Food Sci. Technol.* **2011**, *46*, 1329. [Crossref]
12. Guinee, T. P.; *Int. J. Dairy Technol.* **2004**, *57*, 99. [Crossref]
13. Cremasco, H.; Galvan, D.; Angilelli, K. G.; Borsato, D.; de Oliveira, A. G.; *Food Sci. Technol.* **2019**, *39*, 173. [Crossref]
14. Bona, E.; Carneiro, R. L.; Borsato, D.; Silva, R. S. S. F.; Fidelis, D. A. S.; Silva, L. H. M.; *Braz. J. Chem. Eng.* **2007**, *24*, 337. [Crossref]
15. Angilelli, K. G.; Orives, J. R.; da Silva, H. C.; Coppo, R. L.; Moreira, I.; Borsato, D.; *J. Food Process. Preserv.* **2015**, *39*, 329. [Crossref]
16. Clemente, M. A. J.; de Oliveira, T. F.; Cremasco, H.; Galvan, D.; Bordin, M. S. P.; Moreira, I.; Borsato, D.; *Heat Mass Transfer* **2020**, *56*, 2203. [Crossref]
17. Cremasco, H.; Borsato, D.; Angilelli, K. G.; Galão, O. F.; Bona, E.; Valle, M. E.; *J. Sci. Food Agric.* **2016**, *96*, 306. [Crossref]
18. Haykin, S.; *Neural Networks: A Comprehensive Foundation*, 2nd ed.; Preditice Hall: New Jersey, 2001.

19. Mattos, J. B.; Cruz, M. J. M.; de Paula, F. C. F.; Sales, E. F.; *Eng. Sanit. Ambiental* **2019**, *24*, 501. [Crossref]

20. Bona, E.; da Silva, R. S. S. F.; Borsato, D.; Bassoli, D. G.; *Acta Sci., Technol.* **2012**, *34*, 111. [Crossref]

21. Borsato, D.; Pina, M. V. R.; Spacino, K. R.; Scholz, M. B. S.; Androcioli Filho, A.; *Eur. Food Res. Technol.* **2011**, *233*, 533. [Crossref]

22. Lemes, M. R.; Dal Pino, A.; *J. Chem. Educ.* **2011**, *88*, 1511. [Crossref]

23. Lindsey, R.; Daluiski, A.; Chopra, S.; Lachapelle, A.; Mozer, M.; Sicular, S.; Hanel, D.; Gardner, M.; Gupta, A.; Hotchkiss, R.; Potter, H.; *Proc. Natl. Acad. Sci.* **2018**, *115*, 11591. [Crossref]

24. Walkoff, A. R.; Antunes, S. R. M.; Arrúa, M. E. P.; Silva, L. R. C.; Borsato, D.; Rodrigues, P. R. P.; *Orbital: Electron. J. Chem.* **2017**, *9*, 248. [Crossref]

25. Kohonen, T.; *Self Organizing Maps (Series in Information Sciences)*, 2nd ed.; Springer: Heidelberg, 1997.

26. Boishebert, V.; Giraudel, J. L.; Montury, M.; *Chemom. Intell. Lab. Syst.* **2006**, *80*, 13. [Crossref]

27. Oliveira, T. F.; Clemente, M. A. J.; Galvan, D.; Fix, G.; Mantovani, A. C.; Borsato, D.; *Food Sci. Technol.* **2020**, *40*, 482. [Crossref]

28. Onsager, L.; *Ann. N. Y. Acad. Sci.* **1945**, *46*, 241. [Crossref]

29. *COMSOL Multiphysics®, version 5.2*; COMSOL, Inc., Burlington, MA, USA, 2016.

30. *Matlab®, version 7b*; The MathWorks Inc., Natick, MA, USA, 2007.

31. Clemente, M. A. J.; Silva, H. H. P.; Silva, N. F.; Campos, J. W.; de Sousa, E. G.; Silva, H. C.; Mantovani, A. C. G.; Angilelli, K. B.; Borsato, D.; *Quim. Nova* **2023**, *46*, 229. [Crossref]

32. Lide, D. R.; Frederikse, H. P.; *Handbook of Chemistry and Physics*, 78th ed.; CRC Press: Boca Raton, 1997.